Preparation of NdCrO$_3$ nanoparticles and their catalytic activity in the thermal decomposition of ammonium perchlorate by DSC/TG-MS

Zongxue Yu · Yuxi Sun · Wenxian Wei ·
Lude Lu · Xin Wang

Abstract Orthorhombic structural perovskite NdCrO$_3$ nanocrystals with size of 60 nm were prepared by microemulsion method, and characterized by XRD, TEM, HRTEM, SEM, EDS and BET. The catalytic effect of the NdCrO$_3$ for thermal decomposition of ammonium perchlorate (AP) was investigated by DSC and TG-MS. The results revealed that the NdCrO$_3$ nanoparticles had effective catalysis on the thermal decomposition of AP. Adding 2% of NdCrO$_3$ nanoparticles to AP decreased the temperature of thermal decomposition by 87° and increased the heat of decomposition from 590 to 1073 J g^{-1}. Gaseous products of thermal decomposition of AP were NH$_3$, H$_2$O, O$_2$, HCl, N$_2$O, NO, NO$_2$ and Cl$_2$. The mechanism of catalytic action was based on the presence of superoxide ion O$_2^-$ on the surface of NdCrO$_3$, and the difference of thermal decomposition of AP with 2% of NdCrO$_3$ and pure AP was mainly caused by the different extent of oxidation of ammonium.

Keywords NdCrO$_3$ nanoparticles · Ammonium perchlorate · Catalytic activity · Thermal decomposition · Thermogravimetry-mass spectrometry

Introduction

The vast majority of catalysts used in modern chemical industry is based on mixed metal oxides. Among the mixed metal oxides, ABO$_3$ perovskite-type oxides with A as La, B as transition metal were considered strategic materials due to their prominent electronic, magnetic, optic, catalytic activities and application in many fields [1–4]. In ACrO$_3$ (A = La, Y, Nd and Sm) perovskite system, many investigations have been focused on pure and doped materials of the former two. ACrO$_3$ has been prepared by various techniques: a solid-state reaction [5, 6], a coprecipitation method [7], a simultaneous crystallization method [7], a citric gel processing [8], and a combustion synthesis [9, 10].

Ammonium perchlorate (AP) is the most common oxidizer in composite solid propellants. The thermal decomposition characteristics influence the combustion behavior of the propellant [11]. The catalytic activities of some transition metal oxides and metal powders in the thermal decomposition of AP have been reported [12–17] and improved catalytic performance can be obtained from nanometer-scale catalysts [18–20]. We previously reported the catalytic activities of the perovskite-type oxides nanoparticles for the thermal decomposition of AP [21]. The aim of this work was to investigate the catalytic activities of NdCrO$_3$ nanocrystals prepared by the microemulsion method on the thermal decomposition of AP. The emphasis of the work is on the mechanism of the process studied by DSC and TG-MS technique.

Experimental

Materials

All the reagents were analytical grade chemicals. Cr(NO$_3$)$_3$ · 9H$_2$O, Nd$_2$O$_3$ and sodium dodecylbenzenesulfonate were obtained from the Shanghai Chemical Factory; HNO$_3$, ethanol and toluene were produced by the Nanjing chemical factory.

Z. Yu · Y. Sun · W. Wei · L. Lu (✉) · X. Wang
Key Laboratory of Educational Ministry for Soft Chemistry
and Functional Materials, Nanjing University of Science
and Technology, Nanjing 210094, Jiangsu, China
e-mail: haiqingy@163.com

Z. Yu
Department of Chemical Engineering, Chongqing Three Gorges
College, Wanzhou, 404000 Chongqing, China

Preparation of NdCrO₃ nanoparticles

NdCrO₃ nanoparticles were synthesized through the formation of water-in-toluene reverse micelles with sodium

dodecylbenzenesulfonate $[CH_3(CH_2)_{11}(C_6H_4)SO_3]Na$ (NaDBS) as surfactant. The synthesis starts with 0.005 mol of Nd_2O_3 (dissolved in 1:1 HNO_3) and 0.01 mol of $Cr(NO_3)_3$ dissolved in 25 mL of water to form a clear solution. A 0.4 M NaDBS aqueous solution (25 mL) was added into the metal salt solution and followed by the addition of a large volume
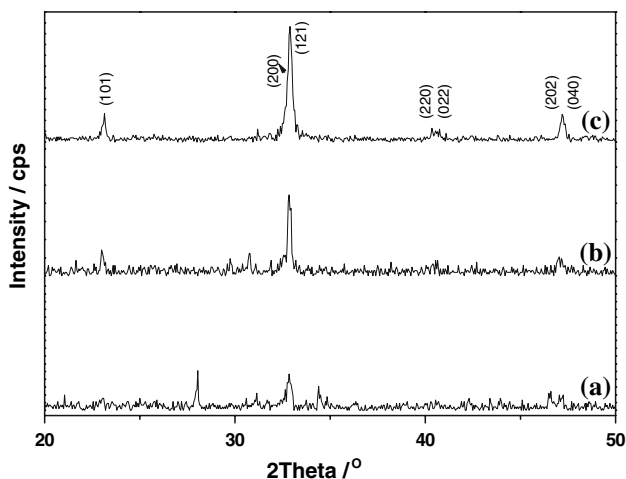

Fig. 1 XRD pattern of the NdCrO₃ calcined at different temperature for 4 h (a) 700 °C; (b)800 °C; (c) 900 °C

Fig. 4 TG and DTG curves for (a) pure AP + NdCrO₃, (b) Pure AP

Fig. 2 TEM and HRTEM images of the NdCrO₃ nanocrystals
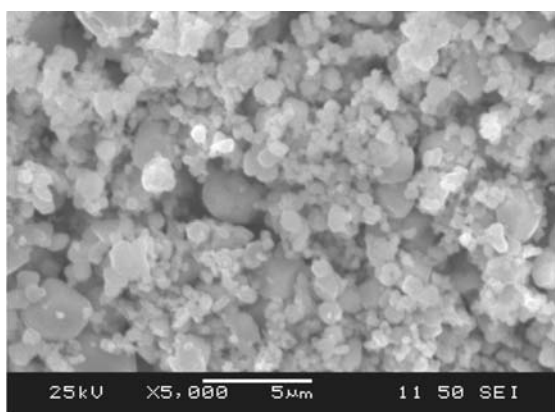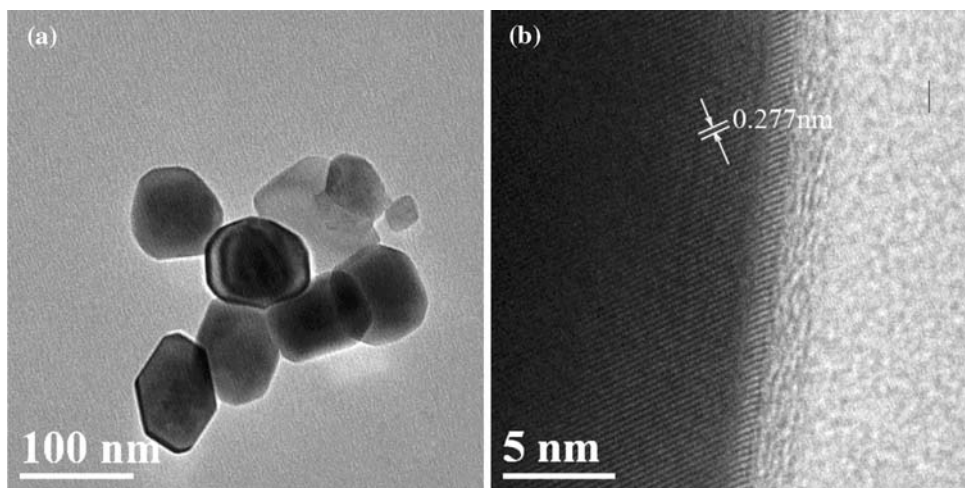
Fig. 3 SEM images and EDS spectrum of the NdCrO₃ nanocrystals

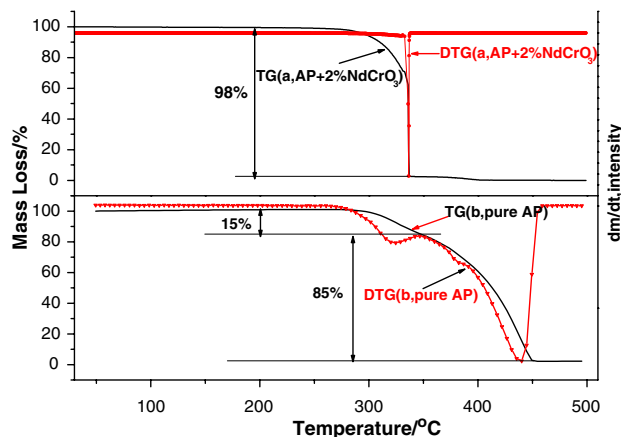| Element	Wt%	At%
C K	04.69	17.75
O K	16.22	46.06
Nd L	58.87	18.54
Cr K	20.21	17.66
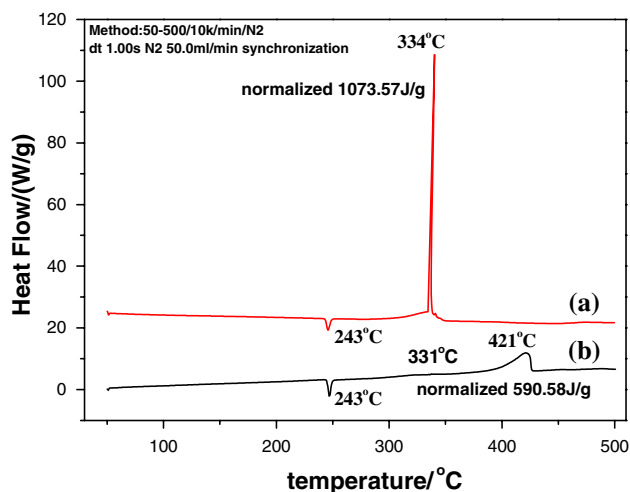
Fig. 5 DSC curves for (a) pure AP + NdCrO₃, (b) pure AP

aqueous solution was added drop by drop accompanied by vigorous stirring. The solution was stirred for more than 2 h to complete the formation of colloids. Then, the volume of the solution was reduced by distilling out water and most of the toluene solvent. The concentrated solution with suspended colloids was washed with water and ethanol to remove excess surfactant. The products were collected through centrifugation. Then, the precursor was calcined at a series of increasing temperatures ranging from 700 to 900 °C for 2 h in air.

NdCrO₃ and AP were mixed in 2:98 (wt%), respectively, to prepare the samples for the thermal analysis.

Instrumentation

X-ray diffraction (XRD) was carried out on a Bruker D8 Advance X-ray diffraction instrument (Cuk$_\alpha$), the diffraction angle (2θ) from 25 to 70° was scanned. Transmission electron microscopy (TEM) images were taken with a JEM-200CX electron microscope, the sample was dispersed in aqueous ethanol by ultrasonic stirring. The BET

of toluene. After stirring overnight, the mixture became a clear single-phase solution containing reverse micelles. To form colloids in reverse micelles, 40 mL of 1.5 M NaOH
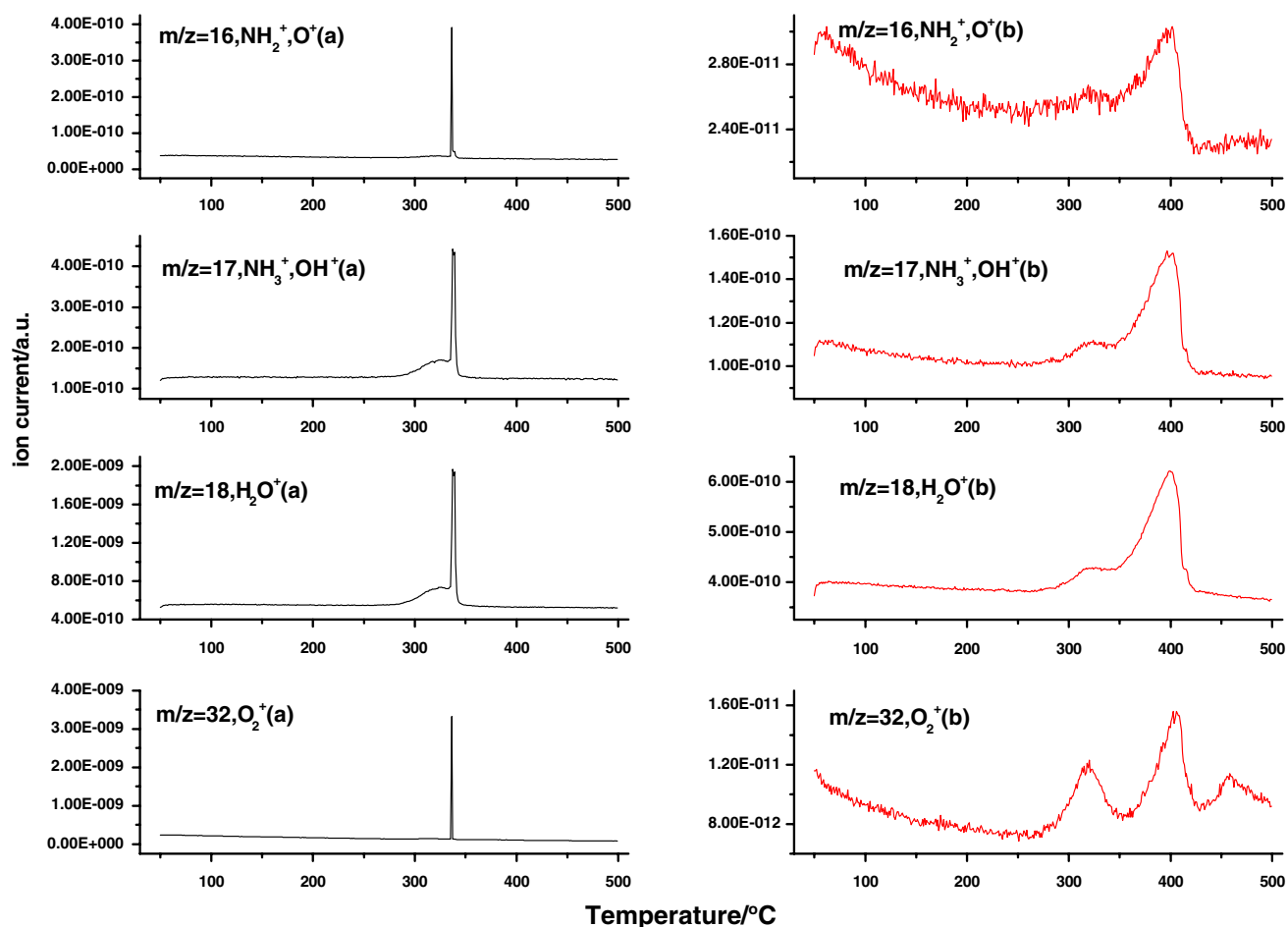

Fig. 6 Ion current versus temperature curves of ion fragments of NH₃, H₂O and O₂ (m/z 16, 17, 18, 32) during the thermal decomposition of NH₄ClO₄ evolved from (a) pure AP + 2% NdCrO₃ (1.5600 mg), (b) pure AP (1.5700 mg)
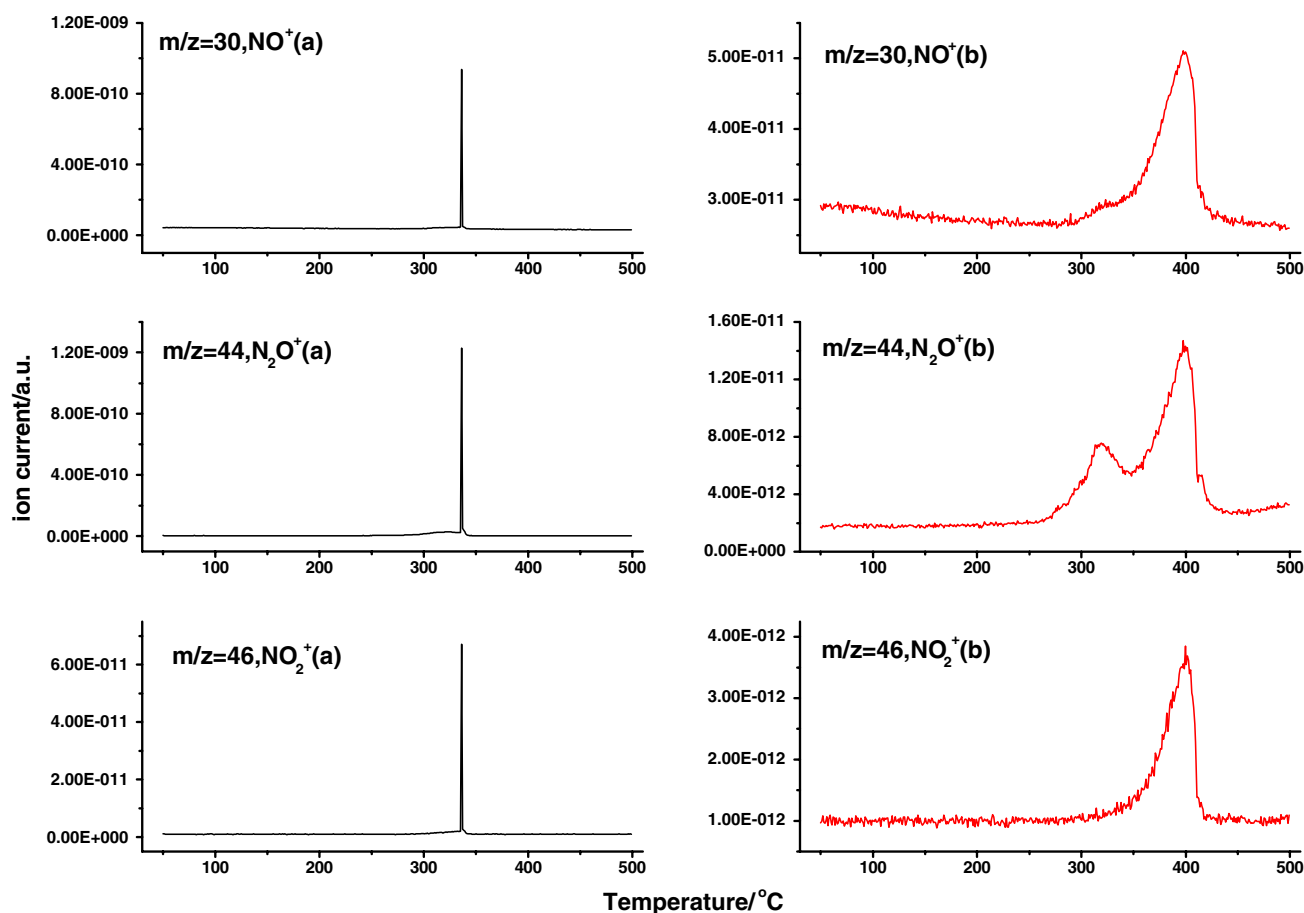
Fig. 7 Ion current versus temperature curves of ion fragments of NO, N₂O and NO₂ (m/z 30, 44, 46) during the thermal decomposition of NH₄ClO₄ evolved from (a) pure AP + 2% NdCrO₃ (1.5600 mg), (b) pure AP (1.5700 mg)

surface areas were measured on an ASAP 2020 instrument using N_2 adsorption at −196 °C.

Thermal decomposition characteristics of the sample were determined by a simultaneous thermal analyzer (Mettler Toledo, model TGA/SDTA 851e) coupled on line with a quadrupole mass spectrometry (Pfeiffer Vacuum, model Thermostar GSD301T3), under the condition of flowing argon gas (purity, 99.999%; flowing rate, 50 mL min⁻¹; atmospheric pressure) at the heating rate of 10 °C min⁻¹ when the sample quantum was about 1.00 mg with Al_2O_3 as reference. The connection between the thermobalance and the mass spectrometer was done by means of a stainless steel capillary, maintained at 150 °C. The mass spectrometer was operated with an electron impact ionizer with energy 70 eV and the intensities of the m/z ranging from 12 to 100 were monitored. DSC823E (Mettler Toledo) was used at a heating rate of 20 °C/min in N_2 atmosphere over the range 20–500 °C, and all samples were placed in aluminum pans with lids.

Results and discussion

NdCrO₃ samples characterization

The $NdCrO_3$ product was characterized by XRD, TEM, SEM and EDS. The XRD measurement (Fig. 1c) shows the product is pure perovskite oxide $NdCrO_3$ (900 °C) with an orthorhombic structure, and the diffraction data are in good agreement with JCPDS card of $NdCrO_3$ (JCPDS no.: 71-1274). No impure peaks are observed in the XRD pattern. The average particle size is 56 nm determined from the XRD pattern parameters of the $NdCrO_3$ powder according to the Scherrer equation.

The TEM image in Fig. 2a shows practically monodisperse particles with an average size of about 60 nm, which is consistent with the average size obtained from the peak broadening in X-ray diffraction studied. A typical HRTEM image is presented in Fig. 2b, showing that the nanoparticles exhibit clearly resolved lattice fringes with the interplanar
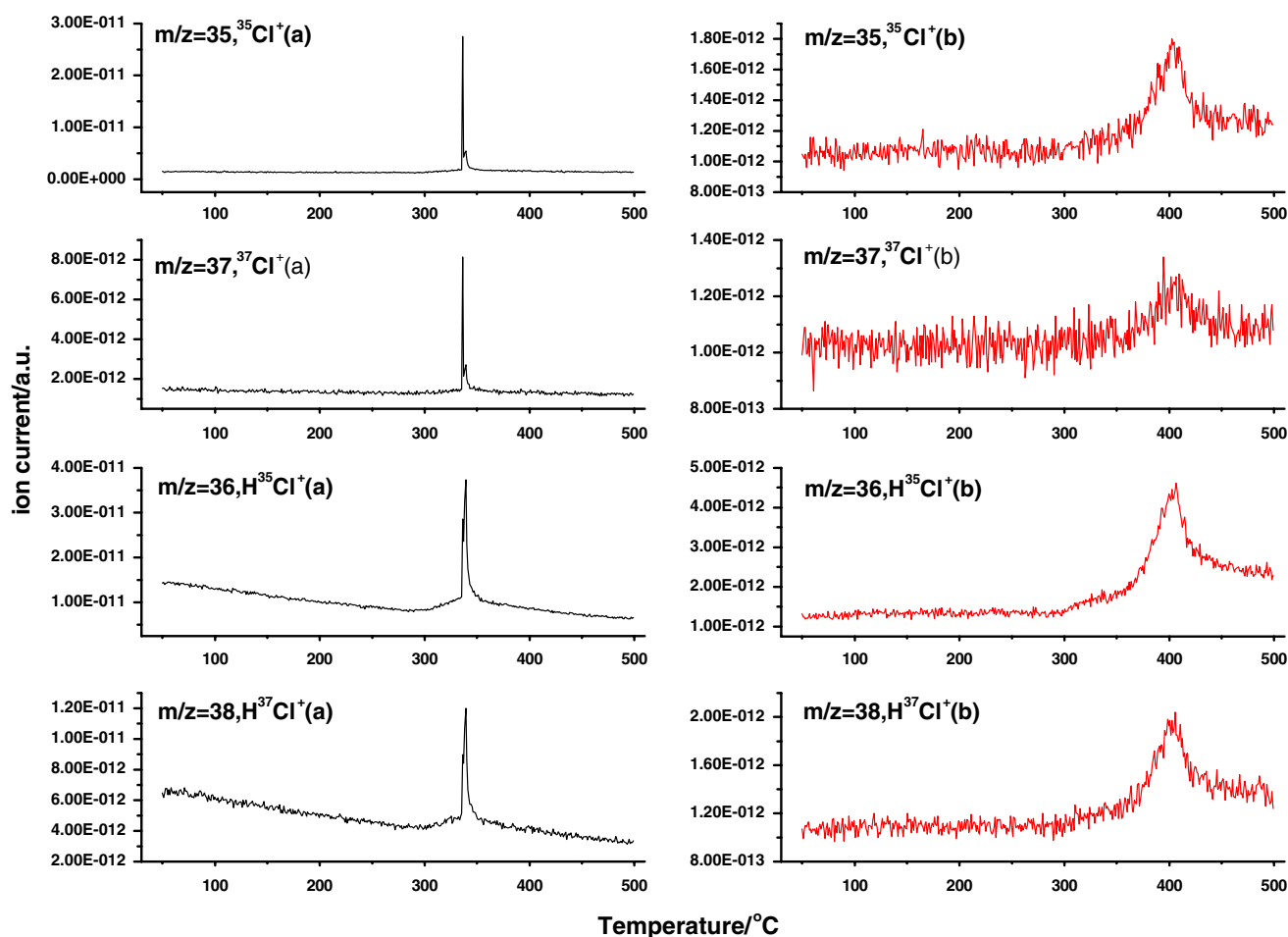
Fig. 8 Ion current versus temperature curves of ion fragments of H^{35}Cl and H^{37}Cl (m/z 36, 36, 37, 38) during the thermal decomposition of NH$_4$ClO$_4$ evolved from (a) pure AP + 2% NdCrO$_3$ (1.5600 mg), (b) pure AP (1.5700 mg)

spacing of 0.277 nm assigned to the (121) plane of the orthorhombic NdCrO$_3$ structure.

Scanning electron micrographs shown in Fig. 3 reveal the product is a low density, loose and porous material that is favorable to the catalytic application. EDS was performed to further confirm the composition of as-prepared products. Figure 3b shows that the products are composed of Nd, Cr and O with a mol ratio of 1:1:3, giving a stoichiometric formula of NdCrO$_3$. The C peak in the spectrum is attributed to the electric latex of the SEM sample holder. Based on the XRD, TEM, EDS analysis, the structure of NdCrO$_3$ nanoparticles was obtained. The BET surface area of NdCrO$_3$ nanocrystals calculated from N$_2$ isotherms at −196° are 10.07 m^2/g.

Catalytic effect

The results of the DSC and TG experiments are shown in Figs. 4 and 5, respectively.

The first endothermic DSC peak with a peak temperature of 242 °C is accompanied with zero weight loss. The additives have no effects on the crystallographic transition temperature which represents the transition from orthorhombic to cubic AP [12]. Figures 4b and 5b are the TG, DTG and DSC curves of pure AP. The first exothermic peak with a peak temperature of 331 °C corresponding 15% weight loss is attributed to the partial decomposition of AP and the formation of some intermediate NH$_3$ and HClO$_4$ by dissociation and sublimation [12, 22–24]. The second exothermic DSC peak with a peak temperature of 421 °C associated with 85% weight loss is caused by the complete decomposition of the intermediate to volatile products [12].

Figures 4a and 5a are the TG, DTG and DSC curves of AP in presence of NdCrO$_3$ catalysts. The experiment results indicate that NdCrO$_3$ has strong catalytic activity on the thermal decomposition of AP. The first exothermic peak at 334 °C becomes a sharp one which is associated
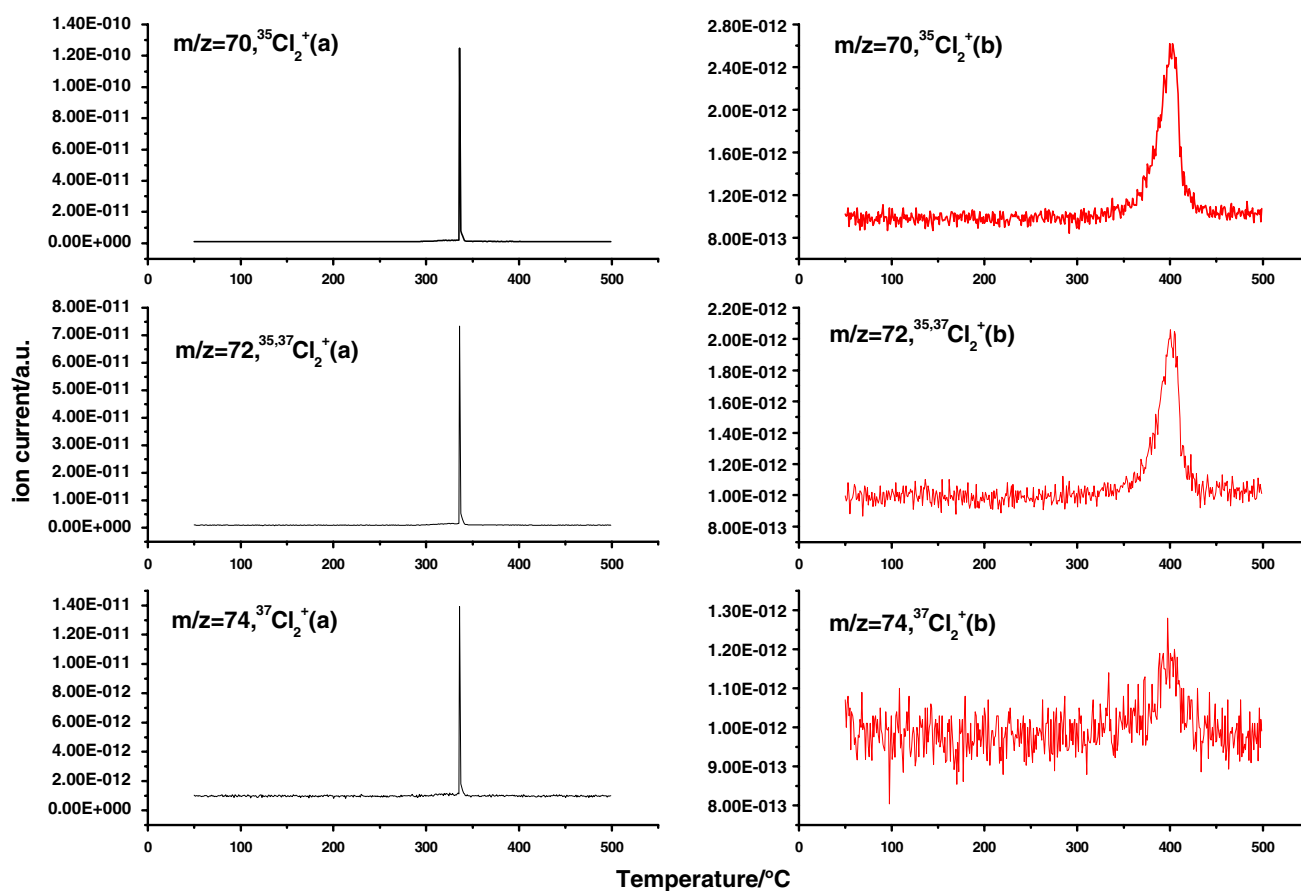
Fig. 9 Ion current versus temperature curves of ion fragments of $^{35}Cl_2$, $^{36,37}Cl_2$ and $^{37}Cl_2$ (m/z 70, 72, 74) during the thermal decomposition of NH_4ClO_4 evolved from (a) pure AP + 2% $NdCrO_3$ (1.5600 mg), (b) pure AP (1.5700 mg)

with only one step weight loss on the TG curve. The second exothermic peak is absent. The addition of $NdCrO_3$ decreases the decomposition temperature of AP and increases the weight loss rate as well as heat of decomposition reaction. It can be found that adding 2% of $NdCrO_3$ nanoparticles to AP decreases the temperature of thermal decomposition by 87 °C and increases the heat of decomposition from 590 to 1073 J g^{-1}.

The results of the TG-MS experiments are shown in Figs. 6, 7, 8, and 9. The TG curve has clear association to the MS curve. The detection of HCl, H_2O, N_2O, NH_3, Cl_2, NO, O_2, NO_2, NH_2^+ and O^+ ion are observed. The difference between decomposition of pure AP and AP with 2% $NdCrO_3$ is shown in Figs. 6, 7, 8, and 9.

Figures 6, 7, 8, and 9b shows the TG-MS of pure AP. The gaseous products of thermal decomposition are formed in two steps. At low-temperature, products of thermal decomposition of pure AP are NH_3, H_2O and a small amount of N_2O, O_2. At the high-temperature stage, HCl, H_2O, N_2O, NH_3, Cl_2, NO, O_2, NO_2 and a small amount of ClO_2 are formed.

Figures 6, 7, 8, and 9a show the intensity curves of ion currents evolved during the thermal decomposition of AP in

presence of $NdCrO_3$. AP is completely decomposed in lower temperature and shorter time. Compared with the decomposition of pure AP, the gaseous products are instantly formed in one step with the catalysis of $NdCrO_3$. The products of thermal decomposition detected are HCl, H_2O, N_2O, NH_3, Cl_2, NO, O_2 and NO_2. ClO_2 is not detected.

Analysis on the mechanism of thermal decomposition of AP

Figure 5 shows the change of the decomposition heat for pure and catalyzed AP. The sharp exothermic peak shown in the DSC curves in Fig. 5a, which is indicative of rapid chemical reaction, are confirmed by TG and MS analysis. The catalytic activity is dependent on the specific surface area of $NdCrO_3$. It is known the nanocrystalline can produce large numbers of the reaction active center. Due to the specific surface and more reaction active centers of $NdCrO_3$ nanoparticles, it is beneficial for the adsorption of O_2 on the surface of $NdCrO_3$ [25]. Therefore, nanosized $NdCrO_3$ should be considered to be the catalyst accelerating both the decomposition of perchloric acid and oxidation of ammonia.

The mechanism of catalytic action is based on the presence of superoxide ion (O$_2^-$) on the surface of NdCrO$_3$ [25, 26]. During the thermal decomposition of AP, the O$_2^-$ ions, which are formed from the oxygen adsorbed on the surface of the oxide, are proton traps, and they can simplify thermal decomposition of AP. The oxidation reaction of ammonia is happened by the collision between ammonia and the oxygen absorbed on the surface of NdCrO$_3$. Increasing the partial pressure of oxygen, the formation of O$_2^-$ covered sites on NdCrO$_3$ are increased, and then the presence of oxygen can accelerate the thermal decomposition process of AP as well as the oxidation of NH$_3$ which increases the exothermic heat of the thermal decomposition process. Figure 7 (m/z = 30, 44, 46) show that the mass spectrometric ion intensities of nitrogen oxides (NO, N$_2$O, NO$_2$) are bigger than those during the thermal decomposition of pure AP.

Conclusions

NdCrO$_3$ nanocrystals synthesized by microemulsion has an orthorhombic structure with an average size of 60 nm. Adding 2% of NdCrO$_3$ to AP can decrease the decomposition temperature by 87 °C and increase the heat of decomposition by 0.4 kJ g^{-1}. AP was completely decomposed in lower temperature and shorter time.

The mechanism of catalytic action is based on the presence of superoxide ion O$_2^-$ on the surface of NdCrO$_3$. The oxidation of adsorbed ammonia by NdCrO$_3$ via the superoxide active centers takes place on the surface of NdCrO$_3$. Therefore, the difference of thermal decomposition of AP with 2% of NdCrO$_3$ and pure AP is mainly caused by the different extent of oxidation of ammonium, which results in the increase of the heat of decomposition with the catalysis of NdCrO$_3$.

References

1. Fernandes JDG, Melo DMA, Zinner LB, Salustiano CM, Silva ZR, Martinelli AE, et al. Low-temperature synthesis of single-phase crystalline LaNiO$_3$ perovskite via Pechini method. Mater Lett. 2002;53:121–5.
2. Peňa MA, Fierro JLG. Chemical structures and performance of perovskite oxides. Chem Rev. 2001;101:1981–2017.
3. Skinner SJ. Recent advances in Perovskite-type materials for solid oxide fuel cell cathodes. Int J Inorg Mater. 2001;3:113–21.
4. Norman AK, Morris MA. The preparation of the single-phase perovskite LaNiO$_3$. J Mater Process Technol. 1999;92–93:91–6.
5. McCarthy GJ, Gallagher PV, Sipe C. Crystal chemistry of catalyst materials. I. Composition and unit cell parameters of "REMnO$_3$" phases prepared in air. Mater Res Bull. 1973;8:1277–84.
6. Savchenko VF, Rubinchik IaS. Study of the reaction of formation of neodymium chromite from oxides. Neorg Mater. 1979;15:122–4.
7. Galdón A, Guillem MC. Preparation of mixed oxides MNdO$_3$, with M=Cr,Fe. Comparison of several methods. Solid State Ionics. 1993;63:66–70.
8. Devi PS. Citrate gel processing of the perovskite lanthanide chromites. J Mater Chem. 1993;3:373–9.
9. Kingsley JJ, Pederson LR. Combustion synthesis of perovskite LnCrO$_3$ powders using ammonium dichromate. Mater Lett. 1993;18:89–96.
10. Manoharan SS, Patil KC. Combustion route to fine particle perovskite oxides. J Solid State Chem. 1993;102:267–76.
11. Survase DV, Gupta M, Asthana SN. The effect of Nd$_2$O$_3$ on thermal and ballistic properties of ammonium perchlorate based compostite propellants. Prog Cryst Growth Charact Mater. 2002;32:161–5.
12. Said AA, AI-Qusmi R. The role of copper cobaltite spinal, Cu$_x$Co$_3$-xO$_4$ during the thermal decomposition of ammonium perchlorate. Thermochim Acta. 1996;275:83–91.
13. Zhi J, Tian-Fang W, Shu-Fen L, Feng-Qi Z, Zi-Ru L, Cui-Mei Y, et al. Thermal behavior of ammonium perchlorate and metal powders of different grades. J Therm Anal Calorim. 2006;85:315–20.
14. Chen LJ, Li GS, Qi P, Li LP. Thermal decomposition of ammonium perchlorate activated via addition of NiO nanocrystals. J Therm Anal Calorim. 2008;92(3):765–9.
15. Chen LJ, Li GS, Li LP. CuO nanocrystals in thermal decomposition of ammonium perchlorate stabilization, structural characterization and catalytic activities. J Therm Anal Calorim. 2008;91(3):581–7.
16. Su YL, Li SF, Ding DH. Effect of ammonium oxalate/strontium carbonate on the burning rate characteristics of composite propellants. J Therm Anal Calorim. 2006;86:497–503.
17. Singh NB, Ojha AK. Formation of copper oxide through NaNO$_3$–KNO$_3$ eutectic melt and its catalytic activity in the decomposition of ammonium perchlorate. Thermochim Acta. 2002;390:67–72.
18. Zhu J, Chen H, Xie B, Yang X, LU L, Wang X. Preparation of nanocrystalline Cu$_2$O and its catalytic performance for thermal decomposition of ammonium perchlorate. Chin J Catal. 2004;25:637–40.
19. Zhu W, Zhang WG, Wang HZ, Yang XJ, Lu LD, Wang X. Synthesis and properties of shape-controlled CuO nanocrystals. Chin J Inorg Chem. 2004;20:863–7.
20. Ma Z, Li F, Chen A, Bai H. Preparation and thermal decomposition behavior of Fe$_2$O$_3$/ammonium perchlorate composite nanoparticles. Acta Chimi Sin. 2004;13:1252–5.
21. Wang YP, Yang XJ, Lu LD, Wang X. Experimental study on preparation of LaMO$_3$ (M=Fe, Co, Ni) nanocrystals and their catalytic activity on NH$_4$ClO$_4$ decomposition. Thermochim Acta. 2006;443:234–39.
22. Rosser WA, Inami SH. Thermal decomposition of ammonium perchlorate. Combust Flame. 1968;12:427–35.
23. Jacobs PWM, Pearson GS. Mechanism of the decomposition of ammonium perchlorate. Combust Flame. 1969;13:419–30.
24. Jacobs PW, Russel-Jones A. Sublimation of ammonium perchlorate. Phys Chem. 1968;72:202–7.
25. Seiyama T, Egashira M, Iwamoto M. Some Theoretical problem of Catalysis. Tokyo: University of Tokyo Press; 1973. p. 35.
26. Johnstone HF, Houvouras ET, Schowalter WR. Ind Eng Chem. 1954;46:702–8.